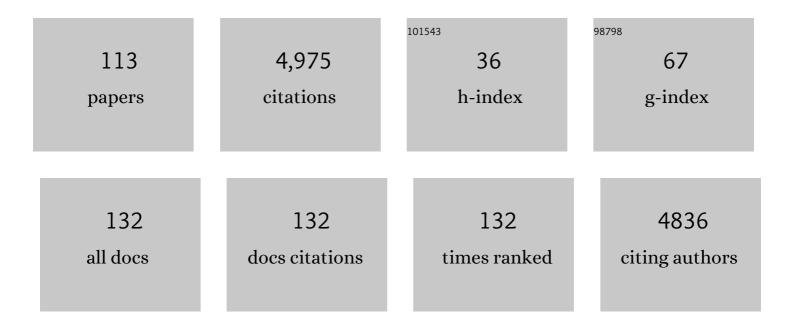
Michael Kersten

List of Publications by Year in descending order

Source: https://exaly.com/author-pdf/5451717/publications.pdf Version: 2024-02-01



#	Article	IF	CITATIONS
1	Real-time 3D imaging of Haines jumps in porous media flow. Proceedings of the National Academy of Sciences of the United States of America, 2013, 110, 3755-3759.	7.1	490
2	Chemical Fractionation of Heavy Metals in Anoxic Estuarine and Coastal Sediments. Water Science and Technology, 1986, 18, 121-130.	2.5	299
3	Three-Dimensional Trace Element Analysis by Confocal X-ray Microfluorescence Imaging. Analytical Chemistry, 2004, 76, 6786-6791.	6.5	237
4	Microstructural evolution of gas hydrates in sedimentary matrices observed with synchrotron <scp>X</scp> â€ r ay computed tomographic microscopy. Geochemistry, Geophysics, Geosystems, 2015, 16, 1711-1722.	2.5	208
5	From connected pathway flow to ganglion dynamics. Geophysical Research Letters, 2015, 42, 3888-3894.	4.0	204
6	Normalization procedures for sediment contaminants in spatial and temporal trend monitoring. Journal of Environmental Monitoring, 2002, 4, 109-115.	2.1	154
7	Aqueous Solubility Diagrams for Cementitious Waste Stabilization Systems: II, Endâ€Member Stoichiometries of Ideal Calcium Silicate Hydrate Solid Solutions. Journal of the American Ceramic Society, 2001, 84, 3017-3026.	3.8	147
8	Mn, Fe, Zn and As speciation in a fast-growing ferromanganese marine nodule. Geochimica Et Cosmochimica Acta, 2004, 68, 3125-3136.	3.9	142
9	Effect of sample pretreatment on the reliability of solid speciation data of heavy metals — implications sesfor the study of early diagenetic processes. Marine Chemistry, 1987, 22, 299-312.	2.3	119
10	Fast X-ray Micro-Tomography of Multiphase Flow in Berea Sandstone: A Sensitivity Study on Image Processing. Transport in Porous Media, 2014, 105, 451-469.	2.6	115
11	Connected pathway relative permeability from pore-scale imaging of imbibition. Advances in Water Resources, 2016, 90, 24-35.	3.8	113
12	Leaching behaviour and solubility — Controlling solid phases of heavy metals in municipal solid waste incinerator ash. Waste Management, 1996, 16, 129-134.	7.4	103
13	Polycyclic aromatic hydrocarbons (PAHs) and their oxygen-containing derivatives (OPAHs) in soils from the Angren industrial area, Uzbekistan. Environmental Pollution, 2010, 158, 2888-2899.	7.5	93
14	Detection of a Ca-rich lithology in the Earth's deep (>300 km) convecting mantle. Earth and Planetary Science Letters, 2005, 236, 579-587.	4.4	90
15	Sediment Criteria Development. , 1990, , 311-338.		88
16	Early diagenetic processes during Mn-carbonate formation: evidence from the isotopic composition of authigenic Ca-rhodochrosites of the Baltic Sea. Geochimica Et Cosmochimica Acta, 2002, 66, 867-879.	3.9	87
17	Processing of rock core microtomography images: Using seven different machine learning algorithms. Computers and Geosciences, 2016, 86, 120-128.	4.2	80
18	Presence of polycyclic aromatic hydrocarbons in sediments and surface water from Shadegan wetland – Iran: A focus on source apportionment, human and ecological risk assessment and Sediment-Water Exchange. Ecotoxicology and Environmental Safety, 2018, 148, 1054-1066.	6.0	77

#	Article	IF	CITATIONS
19	Artifacts in the Determination of Trace Metal Binding Forms in Anoxic Sediments by Sequential Extraction. International Journal of Environmental Analytical Chemistry, 1993, 51, 187-200.	3.3	73
20	Ba and Ni speciation in a nodule of binary Mn oxide phase composition from Lake Baikal. Geochimica Et Cosmochimica Acta, 2007, 71, 1967-1981.	3.9	73
21	3D simulation of the permeability tensor in a soil aggregate on basis of nanotomographic imaging and LBE solver. Journal of Soils and Sediments, 2012, 12, 86-96.	3.0	73
22	Aqueous Solubility Diagrams for Cementitious Waste Stabilization Systems. 3. Mechanism of Zinc Immobilizaton by Calcium Silicate Hydrate. Environmental Science & Technology, 2002, 36, 2919-2925.	10.0	67
23	Source Apportionment of Pb Pollution in the Coastal Waters of Elefsis Bay, Greece. Environmental Science & Technology, 1997, 31, 1295-1301.	10.0	61
24	On the path to the digital rock physics of gas hydrate-bearing sediments – processing of in situ synchrotron-tomography data. Solid Earth, 2016, 7, 1243-1258.	2.8	56
25	Tracing Anthropogenic Thallium in Soil Using Stable Isotope Compositions. Environmental Science & Technology, 2014, 48, 9030-9036.	10.0	52
26	Trace metal fluxes to ferromanganese nodules from the western Baltic Sea as a record for long-term environmental changes. Chemical Geology, 2002, 182, 697-709.	3.3	51
27	Aqueous Solubility Diagrams for Cementitious Waste Stabilization Systems. 1. The C-S-H Solid-Solution System. Environmental Science & amp; Technology, 1996, 30, 2286-2293.	10.0	48
28	Adsorption mechanism of arsenate by zirconyl-functionalized activated carbon. Journal of Colloid and Interface Science, 2008, 317, 228-234.	9.4	48
29	Natural gas hydrate investigations by synchrotron radiation Xâ€ray cryoâ€tomographic microscopy (SRXCTM). Geophysical Research Letters, 2008, 35, .	4.0	46
30	Partitioning of trace metals released from polluted marine aerosols in coastal seawater. Marine Chemistry, 1991, 36, 165-182.	2.3	45
31	Arsenite adsorption on goethite at elevated temperatures. Applied Geochemistry, 2009, 24, 32-43.	3.0	45
32	Fast-growing, shallow-water ferro-manganese nodules from the western Baltic Sea: origin and modes of trace element incorporation. Marine Geology, 2002, 182, 373-387.	2.1	43
33	Digital rock physics, chemistry, and biology: challenges and prospects of pore-scale modelling approach. Applied Geochemistry, 2021, 131, 105028.	3.0	43
34	Ecotoxicity assessment of natural attenuation effects at a historical dumping site in the western Baltic Sea. Marine Pollution Bulletin, 2005, 50, 446-459.	5.0	42
35	Title is missing!. Aquatic Geochemistry, 2000, 6, 147-199.	1.3	40
36	Mineral precipitation-induced porosity reduction and its effect on transport parameters in diffusion-controlled porous media. Geochemical Transactions, 2015, 16, 13.	0.7	40

#	Article	IF	CITATIONS
37	Speciation of trace metals in leachate from a MSWI bottom ash landfill. Applied Geochemistry, 1997, 12, 675-683.	3.0	38
38	Adsorption of the Herbicide 4-Chloro-2-methylphenoxyacetic Acid (MCPA) by Goethite. Environmental Science & Technology, 2014, 48, 11803-11810.	10.0	38
39	Geochemical characterization of the potential trace metal mobility in cohesive sediments. Geo-Marine Letters, 1991, 11, 184-187.	1.1	36
40	Coupling geochemical, mineralogical and microbiological approaches to assess the health of contaminated soil around the Almalyk mining and smelter complex, Uzbekistan. Science of the Total Environment, 2014, 476-477, 447-459.	8.0	36
41	Determination of 206/207Pb isotope ratios by ICP-MS in particulate matter from the north sea environment. Fresenius' Journal of Analytical Chemistry, 1993, 347, 324-329.	1.5	35
42	Advanced spectroscopic, microscopic, and tomographic characterization techniques to study biogeochemical interfaces in soil. Journal of Soils and Sediments, 2012, 12, 3-23.	3.0	34
43	Surface complexation modeling of arsenate adsorption by akagenéite (β-FeOOH)-dominant granular ferric hydroxide. Colloids and Surfaces A: Physicochemical and Engineering Aspects, 2014, 448, 73-80.	4.7	34
44	Speciation of Cr in Leachates of a MSWI Bottom Ash Landfill. Environmental Science & Technology, 1998, 32, 1398-1403.	10.0	33
45	Aqueous Solubility Diagrams for Cementitious Waste Stabilization Systems. 4. A Carbonation Model for Zn-Doped Calcium Silicate Hydrate by Gibbs Energy Minimization. Environmental Science & amp; Technology, 2002, 36, 2926-2931.	10.0	31
46	Low-Molecular-Weight Organic Acid Complexation Affects Antimony(III) Adsorption by Granular Ferric Hydroxide. Environmental Science & Technology, 2019, 53, 5221-5229.	10.0	31
47	Scavenging and particle residence times determined from 234Th/238U disequilibria in the coastal waters of Mecklenburg Bay. Applied Geochemistry, 1998, 13, 339-347.	3.0	30
48	Isotopes Trace Biogeochemistry and Sources of Cu and Zn in an intertidal soil. Soil Science Society of America Journal, 2013, 77, 680-691.	2.2	30
49	Solubility of Zn(II) in Association with Calcium Silicate Hydrates in Alkaline Solutions. Environmental Science & Technology, 1999, 33, 2296-2298.	10.0	29
50	Speciation and oxidation kinetics of arsenic in the thermal springs of Wiesbaden spa, Germany. Fresenius' Journal of Analytical Chemistry, 2001, 371, 927-933.	1.5	29
51	Microstructure characteristics during hydrate formation and dissociation revealed by X-ray tomographic microscopy. Geo-Marine Letters, 2012, 32, 555-562.	1.1	29
52	Polycyclic aromatic hydrocarbons (PAHs) in soils of an industrial area in semi-arid Uzbekistan: spatial distribution, relationship with trace metals and risk assessment. Environmental Geochemistry and Health, 2021, 43, 4847-4861.	3.4	29
53	Microtomographic Quantification of Hydraulic Clay Mineral Displacement Effects During a CO2 Sequestration Experiment with Saline Aquifer Sandstone. Environmental Science & Technology, 2013, 47, 198-204.	10.0	26
54	Competitive arsenate and phosphate adsorption on α-FeOOH, LaOOH, and nano-TiO2: Two-dimensional correlation spectroscopy study. Journal of Hazardous Materials, 2021, 414, 125512.	12.4	26

#	Article	IF	CITATIONS
55	Silicate adsorption by goethite at elevated temperatures. Chemical Geology, 2009, 262, 336-343.	3.3	25
56	Polycyclic aromatic hydrocarbons and trace metal contamination of coastal sediment and biota from Togo. Journal of Environmental Monitoring, 2011, 13, 2033.	2.1	25
57	Simultaneous segmentation and beam-hardening correction in computed microtomography of rock cores. Computers and Geosciences, 2013, 56, 142-150.	4.2	25
58	Assessment of Metal Mobility in Dredged Material and Mine Waste by Pore Water Chemistry and Solid Speciation. , 1988, , 214-237.		25
59	Microfungal Alkylation and Volatilization of Selenium Adsorbed by Goethite. Environmental Science & Technology, 2010, 44, 129-135.	10.0	24
60	Storm Disturbance of Sediment Contaminants at a Hot-Spot in the Baltic Sea Assessed by234Th Radionuclide Tracer Profiles. Environmental Science & Technology, 2005, 39, 984-990.	10.0	22
61	Simulating permeability reduction by clay mineral nanopores in a tight sandstone by combining computer X-ray microtomography and focussed ion beam scanning electron microscopy imaging. Solid Earth, 2021, 12, 1-14.	2.8	20
62	Geochemistry of Priority Pollutants in Anoxic Sludges: Cadmium, Arsenic, Methyl Mercury, and Chlorinated Organics. , 1988, , 170-213.		20
63	Change of arsenite adsorption mechanism during aging of 2-line ferrihydrite in the absence of oxygen. Applied Geochemistry, 2018, 88, 149-157.	3.0	19
64	The Origin of Non-thermal Fluctuations in Multiphase Flow in Porous Media. Frontiers in Water, 2021, 3, .	2.3	19
65	Cr(VI)/Cr(III) and As(V)/As(III) Ratio Assessments in Jordanian Spent Oil Shale Produced by Aerobic Combustion and Anaerobic Pyrolysis. Environmental Science & Technology, 2011, 45, 9799-9805.	10.0	18
66	Time-lapse 3D imaging by positron emission tomography of Cu mobilized in a soil column by the herbicide MCPA. Scientific Reports, 2018, 8, 7091.	3.3	18
67	Distribution and Fate of Heavy Metals in the North Sea. , 1993, , 300-347.		17
68	Benchmarking conventional and machine learning segmentation techniques for digital rock physics analysis of fractured rocks. Environmental Earth Sciences, 2022, 81, 1.	2.7	16
69	Exothermic adsorption of chromate by goethite. Applied Geochemistry, 2020, 123, 104785.	3.0	15
70	The influence of temperature on selenate adsorption by goethite. Radiochimica Acta, 2013, 101, 413-420.	1.2	14
71	Multi-phase classification by a least-squares support vector machine approach in tomography images of geological samples. Solid Earth, 2016, 7, 481-492.	2.8	14
72	Soil biogeochemical properties of Angren industrial area, Uzbekistan. Journal of Soils and Sediments, 2009, 9, 206-215.	3.0	13

#	Article	IF	CITATIONS
73	Squirt flow due to interfacial water films in hydrate bearing sediments. Solid Earth, 2018, 9, 699-711.	2.8	13
74	Incorporation of trace metals Cu, Zn, and Cd into gypsum: Implication on their mobility and fate in natural and anthropogenic environments. Chemical Geology, 2020, 541, 119574.	3.3	13
75	Relationship Between Microbial Growth and Hydraulic Properties at the Sub-Pore Scale. Transport in Porous Media, 2021, 139, 579-593.	2.6	13
76	Trace metals in humic acids from recent Skagerrak sediments. Marine Pollution Bulletin, 1994, 28, 143-147.	5.0	12
77	Successive development of soil ecosystems at abandoned coal-ash landfills. Ecotoxicology, 2014, 23, 880-897.	2.4	12
78	Silicic acid competes for dimethylarsinic acid (DMA) immobilization by the iron hydroxide plaque mineral goethite. Science of the Total Environment, 2015, 508, 199-205.	8.0	10
79	Trace metal(loid) mobility in waste deposits and soils around Chadak mining area, Uzbekistan. Science of the Total Environment, 2018, 622-623, 1658-1667.	8.0	10
80	Cadmium in the North Sea—a mass balance. Journal of Marine Systems, 1992, 3, 209-224.	2.1	9
81	Analysis of Variance of Porosity and Heterogeneity of Permeability at the Pore Scale. Transport in Porous Media, 2019, 130, 867-887.	2.6	9
82	Predicting breakthrough of vanadium in fixed-bed absorbent columns with complex groundwater chemistries: A multi-component granular ferric hydroxideâ^'vanadateâ^'arsenateâ^'phosphateâ^'silicic acid system. Water Research X, 2020, 9, 100061.	6.1	9
83	Competitive Scavenging of Trace Metals by HFO and HMO during Redox-driven Early Diagenesis of Ferromanganese Nodules (11 pp). Journal of Soils and Sediments, 2005, 5, 37-47.	3.0	8
84	Speciation and Mobility of Arsenic in Agricultural Lime. Journal of Environmental Quality, 2009, 38, 2058-2069.	2.0	8
85	Background Concentrations for Metals in the North Sea: Sediment, Water, Mussels and Atmosphere. , 1994, , 290-316.		8
86	Metal associations in anoxic sediments and changes following upland disposalâ€. Toxicological and Environmental Chemistry, 1986, 12, 313-321.	1.2	7
87	Assessment of Metal Mobility in Sludges and Solid Wastes. , 1990, , 1-41.		7
88	Stop-and-go <i>in situ</i> tomography of dynamic processes – gas hydrate formation in sedimentary matrices. Acta Crystallographica Section A: Foundations and Advances, 2015, 71, s154-s154.	0.1	6
89	Pore scale modelling of calcite cement dissolution in a reservoir sandstone matrix. E3S Web of Conferences, 2019, 98, 05010.	0.5	6
90	Predicting the Breakthrough of Ternary Ca–Uranyl–Carbonate Species in Mineral Water Treated by a Fixed-Bed Granular Ferric Hydroxide Adsorbent. ACS ES&T Water, 2021, 1, 366-375.	4.6	6

#	Article	IF	CITATIONS
91	Combined Effects of Abiotic and Biotic Factors on Heavy Metal Fluxes. , 1994, , 598-619.		6
92	Thorium-234 derived information on particle residence times and sediment deposition in shallow waters of the south-western Baltic Sea. Journal of Marine Systems, 2009, 75, 360-370.	2.1	5
93	3-D imaging and quantification of graupel porosity by synchrotron-based micro-tomography. Atmospheric Measurement Techniques, 2011, 4, 2225-2234.	3.1	5
94	Chronospeciation of uranium released in soil during a long-term DU shell weathering experiment. Journal of Environmental Radioactivity, 2021, 228, 106511.	1.7	5
95	Comment on "Enthalpy of Uranium Adsorption onto Hematite― Environmental Science & Technology, 2021, 55, 3442-3443.	10.0	5
96	Section 1: Sediment quality and impact assessment. Journal of Soils and Sediments, 2007, 7, 197-197.	3.0	3
97	Microstructure of hydrate-bearing sediments and determination of P-wave velocities based on high-resolution synchrotron tomographic data. , 2015, , .		3
98	Stratification Dynamics and Geothermal Potential of a Deep Shaft in the Flooded Wolf Mine, Siegerland/Germany. Mine Water and the Environment, 2019, 38, 325-334.	2.0	3
99	Molecular modeling of MCPA herbicide adsorption by goethite (110) surface in dependence of pH. Theoretical Chemistry Accounts, 2020, 139, 1.	1.4	3
100	A FIB-SEM Study of Illite Morphology in Aeolian Rotliegend Sandstones: Implications for Understanding the Petrophysical Properties of Reservoir Rocks. Clays and Clay Minerals, 2022, 70, 84-105.	1.3	3
101	Upscaling calcite dissolution rates in a tight reservoir sandstone. Environmental Earth Sciences, 2022, 81, .	2.7	3
102	Modeling of Elemental Species. , 2005, , 651-689.		2
103	Speciation of Copper in Enriched Agricultural Lime. Soil Science Society of America Journal, 2011, 75, 509-520.	2.2	2
104	LFER and the Effect of Temperature on Oxyanion Adsorption by Goethite. E3S Web of Conferences, 2019, 98, 10001.	0.5	2
105	Mobility of Cr and V in Spent Oil Shale: Impact of Thermal Treatment. Procedia Earth and Planetary Science, 2013, 7, 413-416.	0.6	1
106	CO2 Injection to a Saline Aquifer Sandstone - Clay Mineral Displacement and Permeability Changes. , 2013, , .		1
107	On the Effect of Image Enhancement Techniques on Digital Rock Physics Results. , 2013, , .		1
108	Cadmium isotope fractionation in an intertidal soil induced by tidal pumping. Environmental Advances, 2022, 8, 100182.	4.8	1

#	Article	IF	CITATIONS
109	Comparison of Micro X-ray Computer Tomography Image Segmentation Methods: Artificial Neural Networks Versus Least Square Support Vector Machine. Lecture Notes in Earth System Sciences, 2014, , 141-145.	0.6	0
110	Applied Geochemistry. , 2021, , 323-326.		0
111	Speziierung von Eisen in Brackwassersedimenten der Ostseebodden. , 2001, , 141-166.		0
112	Methoden der Gewinnung geochemischer Parameter. , 1998, , 107-358.		0
113	Aqueous solubility of Zn incorporated into Mg-Al-layered double hydroxides. Clays and Clay Minerals, 2022, 70, 34-47.	1.3	0